Dynamic Changes in Microtubule Configuration Correlate with Nuclear Migration in the Preblastoderm *Drosophila* Embryo

Jayne Baker,* William E. Theurkauf,‡ and Gerold Schubiger*

*Department of Zoology, University of Washington, Seattle, Washington 98195; ‡Department of Biochemistry and Biophysics, University of California, San Francisco, California 94143-0448

Abstract. *Drosophila* embryogenesis is initiated by a series of syncytial mitotic divisions. The first nine of these divisions are internal, and are accompanied by two temporally distinct nuclear movements that lead to the formation of a syncytial blastoderm with a uniform monolayer of cortical nuclei. The first of these movements, which we term axial expansion, occurs during division cycles 4–6 and distributes nuclei in a hollow ellipsoid underlying the cortex. This is followed by cortical migration, during cycles 7–10, which places the nuclei in a uniform monolayer at the cortex. Here we report that these two movements differ in their geometry, velocity, cell-cycle dependence, and protein synthesis requirement. We therefore conclude that axial expansion and cortical migration are mechanistically distinct, amplifying a similar conclusion based on pharmacological data (Zalokar and Erk, 1976).

We have examined microtubule organization during cortical migration and find that a network of interdigitating microtubules connects the migrating nuclei. These anti-parallel microtubule arrays are observed between migrating nuclei and yolk nuclei located deeper in the embryo. These arrays are present during nuclear movement but break down when the nuclei are not moving. We propose that cortical migration is driven by microtubule-dependent forces that repel adjacent nuclei, leading to an expansion of the nuclear ellipsoid established by axial expansion.

THE control of developmental events is often assumed to be based on regulated gene expression. In many organisms, however, the earliest events of embryogenesis proceed without transcription, and in some cases without translation (Gard et al., 1990; Sluder et al., 1986, 1990). In the syncytial embryos of insects nuclei move in precise temporal and spatial patterns that are coordinated with mitotic divisions and are consistent from embryo to embryo within a species (Strasburger, 1934; Maul, 1967; Zalokar and Erk, 1976; Foe and Alberts, 1983). In *Drosophila*, these nuclear movements are transcription-independent processes (Edgar and Schubiger, 1986). Because these early nuclear movements are essential to normal blastoderm formation but are poorly understood, they are the subject of this investigation.

In *Drosophila*, two temporally distinct nuclear movements, which we refer to as axial expansion and cortical migration, produce a syncytial blastoderm with a uniform monolayer of surface nuclei (see Fig. 1). Axial expansion occurs during division cycles 4 through 6, and transforms an initially spherical mass of nuclei into an ellipsoid evenly underlying the cortex (Scriba, 1964; Zalokar and Erk, 1976). Cortical migration occurs during telophase of cycles 8 and 9. During these stepwise movements the future somatic nuclei migrate from their positions in the ellipsoid toward the periphery, reaching the cortex synchronously at interphase of cycle 10. The future pole cell nuclei migrate slightly ahead of the main body of somatic nuclei (see Fig. 1 *c*), and arrive at the posterior cortex during cycle 9 (Foe and Alberts, 1983).

Axial expansion and cortical migration occur within a single cell, suggesting that the cytoskeleton plays a central role in these nuclear movements. Supporting this hypothesis, inhibitor studies have implicated actin filaments in axial expansion and microtubules in cortical migration (Zalokar and Erk, 1976). Most of the detailed cytological studies of the embryonic cytoskeleton have focused on the surface divisions, which take place after cortical migration (Karr and Alberts, 1986; Warn et al., 1984; Warn and Warn, 1986; Kellogg et al., 1988). However, the precise roles of actin and microtubules during the premigration divisions remain elusive.

To gain insights into the mechanisms of nuclear redistribution in the premigration embryo, we have used differential interference microscopy (DIC)[1] and video recording techniques to analyze nuclear movements in live embryos. We

W. E. Theurkauf's present address is Department of Biochemistry and Cell Biology, State University of New York at Stonybrook, Stonybrook, NY 11794.

Abbreviations used in this paper: AED, after egg deposition; CYH, cycloheximide; DIC, differential interference contrast; PBSTx, PBS + Triton X-100.

have used immunohistochemistry and laser scanning confocal microscopy to examine cytoskeletal organization in fixed embryos. These studies indicate that axial expansion and cortical migration proceed by different mechanisms. Moreover, the observations reported here document that cortical migration coincides with dramatic changes in the microtubule configuration, allowing us to propose a novel mechanism for this movement.

Materials and Methods

Stocks and Egg Collections

We collected eggs from *Drosophila melanogaster* (Sevelen strain) females that were 3–10 days post-eclosion. To eliminate overaged eggs, we conducted precollections as follows: 1 h on fresh food, a 30-min precollection on yeast- and acetic acid–flavored agar plates, then two 15-min precollections on agar plates. We collected synchronized embryos for experiments for 10-min intervals on agar plates and we consider the midpoint of the collection as time zero. Embryos were then dechorionated either in 1:1 bleach and embryo wash (0.5% NaCl [J. T. Baker, Philipsburg, NJ] and 0.03% Triton-X 100 [Sigma Immunochemicals, St. Louis, MO]) or manually dechorionated on double-stick tape.

Time-lapse Video Recording

For the study of nuclear movements in living embryos, we manually dechorionated embryos on double-stick tape, lined them up on double-stick tape, and covered them with 3S Volatef low viscosity oil (Ugine-Kuhlmann, France), which is optimal for imaging and still prevents dehydration for several hours. We viewed them on a Zeiss microscope using Nomarski optics and made time-lapse recordings using a MTI 65 video camera, a Gyyr time-lapse video recorder and a Koyo black and white monitor. We made measurements directly on the screen for studying both posterior and cortical movements.

Embryo Squashing for DNA Staining

We videotaped single embryos until we removed them from the slide when they reached a defined phase of posterior migration. Each embryo was transferred to a fresh slide and placed in a drop of heptane (J. T. Baker) to remove the oil. After popping the embryo with the tungsten needle, we dragged the vitelline membrane across the slide, leaving a trail of smeared yolk and cytoplasm behind it. After the smear dried for a few seconds, we covered it with 4% formaldehyde (J. T. Baker) in PBS for 10 min. Between 1 and 2 min elapsed from the time the embryo was removed from the microscope stage until it was fixed. The smear was subsequently rinsed three times with PBS and stained for 4 min in 1 μg/ml 4′,6-diamidino-2-phenylindole (DAPI) from Sigma Immunochemicals in PBS. We rinsed off the DAPI with 3 washes of PBS and covered the smear in 90% glycerol (J. T. Baker) with 10% 10× PBS, 0.1% n-propyl gallate (Sigma Immunochemicals). This preparation was viewed on a Nikon Microphot fluorescence microscope.

Injections

We performed the embryo injections with a Leitz micromanipulator and a Wild compound microscope, according to Foe and Alberts (1983). We hand-dechorionated the embryos as described above and lined them up on a strip of glue, made from double-stick tape dissolved with heptane, on a coverslip. The embryos were desiccated for 5–7 min, depending on the humidity, then covered with halocarbon oil to prevent further desiccation. The injection needles were drawn-out 50 μl capillary pipettes (Drummond Sci. Co., Broomall, PA). We injected cycloheximide (CYH) (Sigma Immunochemicals) at a concentration of 1 mg/ml (Edgar et al., 1986*b*) in injection buffer (IB) (Weir et al., 1988) and colcemid (Sigma Immunochemicals) at a concentration of 0.5 mM in either IB (Edgar et al., 1987) or in 1 mg/ml CYH. The estimated intracellular concentration is a 50-fold dilution of the injected concentration (Foe and Alberts, 1983).

Fluorescent Conjugation of Histone Antibody

We diluted a monoclonal mouse anti-histone antibody (Chemicon Intl., Inc., Temecula, CA) to 2–3 mg/ml in a coupling buffer (0.1 M sodium carbonate from Sigma Immunochemicals) to make a total volume of 200 μl. To this solution we added 2 μl of 50 mg/ml of 5-(and-6)-carboxytetramethylrhodamine (Molecular Probes, Inc., Eugene, OR), in dimethylformamide (Sigma Immunochemicals). After letting the solution incubate for 60 min at room temperature, we stopped the reaction by adding ethanolamine (Sigma Immunochemicals) to 50 mM. To separate conjugated antibody from free label we ran the solution over a Sephadex G-25 gel filtration column (Pharmacia Fine Chemicals, Piscataway, NJ).

Immunohistochemistry

After dechorionation, the embryos were fixed in equal volumes of 37% formaldehyde and heptane (based on method described by Theurkauf, 1992). We devitellinized the uninjected ones by agitation in a bilayer of heptane and methanol then rinsed and stored them in 100% ethanol at −20°C. For the injected embryos, we hand devitellinized them in PBS using tungsten needles. After devitellinization, we transferred them into PBS + 0.1% Triton X 100 (PBSTx) and dehydrated them through an ethanol series and stored them in 100% ethanol at −20°C. After we rehydrated them into PBSTx, we rinsed the embryos thoroughly in PBSTx. We incubated the embryos in 5% normal goat serum (Cappel Labs., West Chester, PA) in PBSTx for 30 min at room temperature to block nonspecific staining. The embryos were incubated overnight at 4°C in 1:800 mouse monoclonal anti-α-tubulin, from Amersham Corp. (Arlington Heights, IL), in PBSTx. After several rinses in PBSTx, the embryos were incubated for 3–6 h at room temperature, or overnight at 4°C, in 1:100 BODIPY-conjugated goat α-mouse secondary antibody (from Molecular Probes, Inc.). At this point we stained the embryos for DNA, either with DAPI (Yasuda et al., 1991*a*), to be viewed using fluorescent microscopy, or with a rhodamine-conjugated mouse anti-histone antibody, to be viewed using a confocal microscope. We diluted the rhodamine-conjugated histone antibody 1:500 in PBSTx and incubated the embryos overnight at 4°C. After we rinsed the embryos several times in PBS, we rinsed them 2–3 times in 100% methanol then put them in 20 μl of 1:2 Benzol Benzoate:Benzyl Alcohol (Sigma Immunochemicals). We mounted them in this solution under a coverslip shimmed with tape and sealed the coverslip with nail polish.

Confocal Microscopy

We analyzed the mounted embryos with a Biorad 600 confocal microscope. For most of the analyses we generated a series of optical sections, 1 μm apart, through the embryo, known as a Z-series. These optical sections can be "projected," or layered, on top of each other. The confocal images presented here are projections of a maximum of five consecutive sections.

Results

Geometry, Velocity, and Cell Cycle Dependence of Axial Expansion and Cortical Migration

Our initial characterization of the preblastoderm nuclear movements reevaluates the spatial distribution of nuclei during division cycles 1 through 7 (see Fig. 2). Under DIC optics, the energids (nuclei and their surrounding cytoplasm) can be observed in living embryos (see Fig. 3). We have analyzed time-lapse video recordings of live embryos and have measured the domain occupied by the energids at each nuclear division. We define the domain in percent egg length from the posterior-most energid to the anterior-most energid (see Fig. 2).

During the first two cycles the nuclei divide and, since they remain equidistant from one another (Scriba, 1964), expand outward isotopically, as a sphere (Fig. 1 *a*). Also, during these cycles the entire population of nuclei moves posteriorly (Fig. 2). During cycles 4 through 6, nuclei spread out along the anterior–posterior axis (Fig. 1, *a* and *b* and Fig. 2). These movements are asymmetric: The posterior-most nuclei move further along the anterior–posterior axis than the anterior-most nuclei. This axial expansion forms an ellipsoid with the

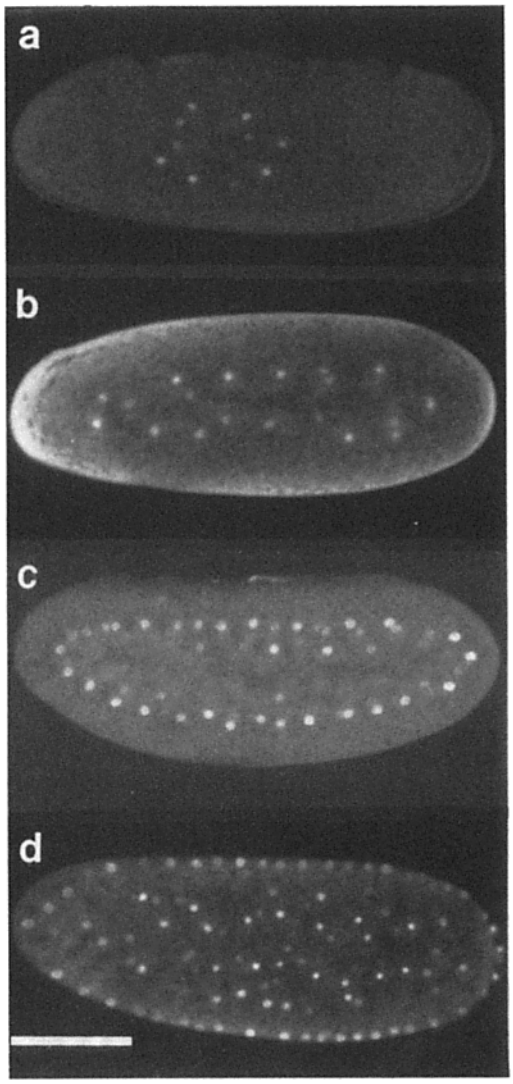

Figure 1. Preblastoderm nuclei undergo two distinct movements. These laser scanning confocal micrographs of embryos labeled with a histone antibody show the location of the nuclei. Between nuclear cycles 4 and 6 (*a*, cycle 5, 52 min; and *b*, cycle 6, 61 min) the nuclei become distributed along the anterior–posterior axis through the process of axial expansion. During cycles 7 through 10 (*c*, cycle 8, 79 min; and *d*, cycle 10, 99 min) nuclei move synchronously toward the surface to form the syncytial blastoderm. We call this process cortical migration. The nuclei remaining in the interior of the embryo are called yolk nuclei. Anterior is left. Times are min AED at room temperature (20°-22°C). Bar, 100 μm.

nuclei in the outer shell equidistant from the cortex (Fig. 1 *b*). Cortical migration, the symmetric outward movement of nuclei from the ellipsoid, occurs during division cycles 7, 8, and 9 (Foe and Alberts, 1983). Because the asymmetric movements of axial expansion position the nuclei uniformly under the cortex, the symmetric movements of cortical migration produce a uniform syncytial blastoderm. Cortical migration and axial expansion therefore differ in geometry.

We have also used DIC analysis of living embryos to determine the velocity of nuclear movements in early embryos. Posterior movement during axial expansion occurs stepwise during 5-min intervals of division cycles 4 and 5. The posterior-most nuclei move a total distance of at least 50 μm

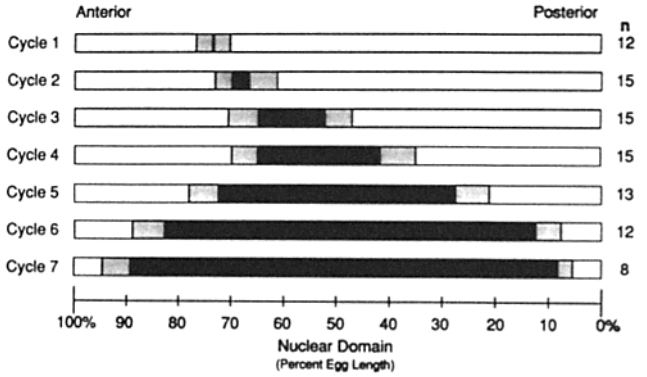

Figure 2. The domain occupied by nuclei enlarges and shifts along the anterior–posterior axis during the first seven nuclear cycles, as observed in video recordings of live embryos. The white bars represent the anterior–posterior axis of the embryo. The solid black region represents the average domain occupied by nuclei at each cycle, denoted in percent egg length. The stippled region indicates the standard deviation in the anterior and posterior boundaries of the domain. *n*, the number of embryos analyzed.

in each cycle ($n = 12$ nuclei, 6 embryos). Each of these periodic movements consists of three phases: an initial slow phase, lasting ~1 min; a fast phase, lasting ~3 min; and a final slow phase of ~1 min, after which the nuclei stop mov-

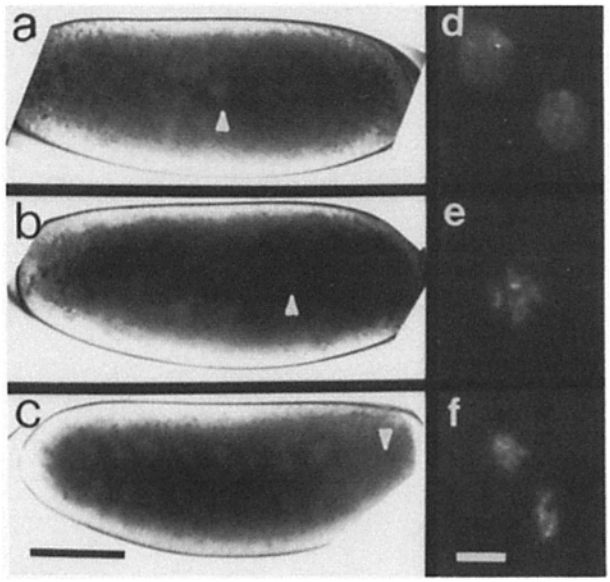

Figure 3. Cell-cycle regulation of axial expansion. We have followed the development of live embryos using DIC microscopy (*a*, *b*, and *c*). Individual embryos at particular stages during the posterior movements of axial expansion were photographed just before fixation and the fixed material was stained with DAPI to reveal nuclear morphology (*d*, *e*, and *f*). The lighter patches in *a* through *c* are the energids. The arrowheads indicate the posterior-most energid. (*a*) An embryo at the initiation of axial expansion and (*d*) DAPI staining of an embryo during this phase, revealing early prophase nuclei. (*b*) An embryo during the rapid phase of posterior movement. (*e*) DAPI staining showing metaphase nucleus of an embryo during this phase. (*c*) An embryo during the final slow phase of posterior movement. (*f*) Anaphase nuclei in an embryo during the final period of movement. The cell-cycle phase of movement has been estimated from this data by correcting for a one to two minute delay between observation and fixation. Anterior is left, dorsal is up. Bars: (*a–c*) 100 μm; (*d–f*) 10 μm.

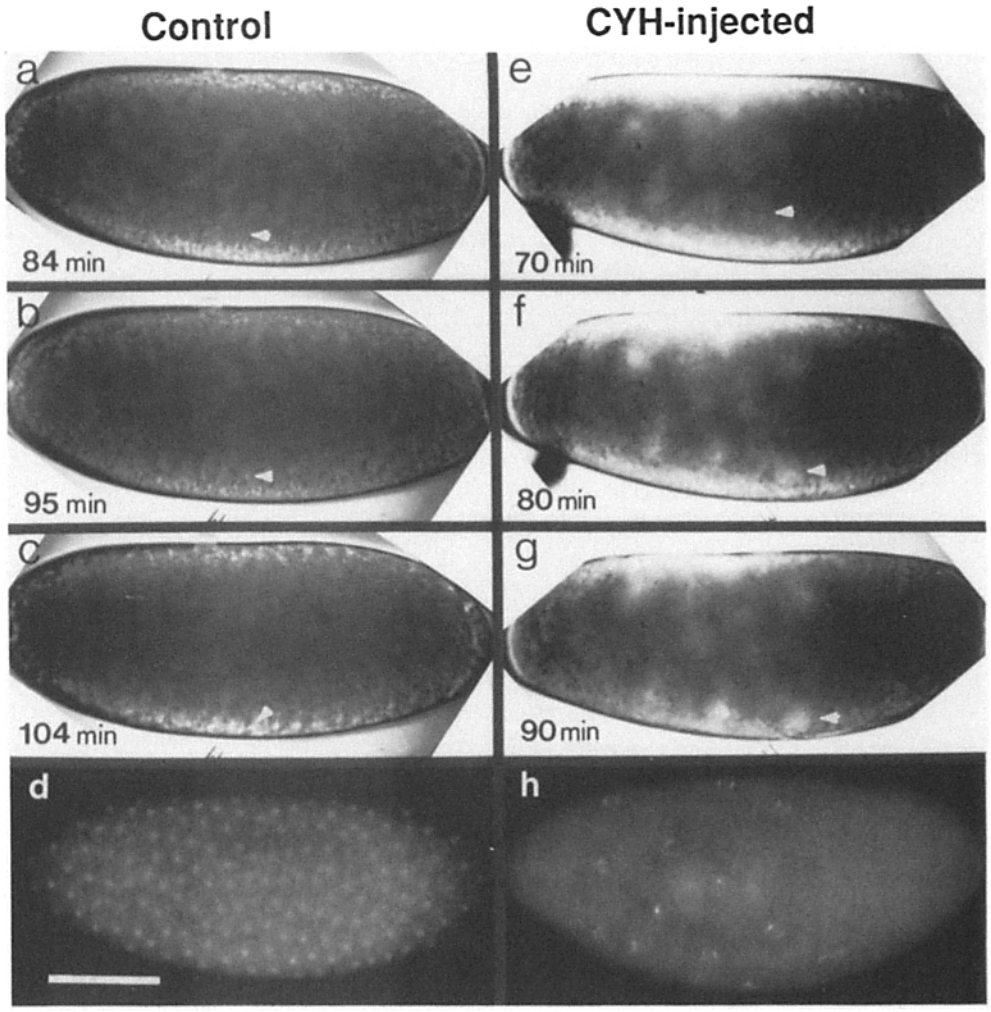

Figure 4. Cortical migration of nuclei in control and cycloheximide injected embryos. *a–c* and *e–g* are sequential video images of single live embryos during cortical migration. Arrowheads indicate representative nuclei in each image. *a–c* are from a control embryo while *e–g* are from an embryo injected with CYH at 45 min AED. *a* and *e* show the early period of cortical migration; *b* and *f* show the continuation of migration; *c* and *g* show the completion of migration. Nuclei in CYH-injected embryos reach the cortex before their control counterparts. Additionally, the nuclei in CYH-injected embryos do not move along the anterior–posterior axis, as the nuclei in control embryos do. This is emphasized in *d* and *h*, which show DAPI staining in a control (*d*) and a CYH-injected (*h*) embryo after the nuclei have reached the cortex. Anterior is left, dorsal is up. Times are min. AED, ±5 min. Bar, 100 μm.

ing. During the fast phase, the posterior-most nuclei move with a mean velocity of 23.2 μm/min (SD = 6.5, n = 23 nuclei, 14 embryos).

Analysis of fixed embryos suggests that the nuclear movements of cortical migration may be significantly slower than the rate of axial expansion (Foe and Alberts, 1983). To directly determine the rate of cortical migration, we have analyzed videotaped sequences of live embryos visualized using DIC microscopy. We found that the average velocity of cortical migration during cycles 8 and 9 is 7.68 μm/min (SD = 3.64, n = 14 nuclei, 5 embryos), and 7.20 μm/min (SD = 1.69, n = 17 nuclei, 6 embryos), respectively. The mean velocity of cortical migration is approximately one third the mean velocity of posterior movement during axial expansion.

Additionally, we have determined the cell-cycle phase during which the posterior movements of axial expansion occur. The preblastoderm cell cycle length (from interphase to interphase) is ~9 min. Interphase lasts ~4.2 min and mitosis is ~4.5 min. The mitotic period can be subdivided into a long prophase (2.0 min), metaphase (1 min), anaphase (1 min), and telophase (0.5 min) (Rabinowitz, 1941; Würgler and Ulrich, 1976). Because posterior movement in live embryos can be observed using DIC optics, we could select individual embryos at specific stages of posterior movement, fix these embryos within 1–2 min, and fluorescently stain them to reveal nuclear morphology (see Materials and Methods). Embryos fixed during the initial slow phase of the movement are in late interphase or prophase (n = 6) (Fig. 3, *a* and *d*), embryos fixed during the fast phase of the movement are in late prophase or metaphase (n = 9) (Fig. 3, *b* and *e*), and embryos fixed during the final slow phase of the movement are in late metaphase, anaphase, or telophase (n = 7) (Fig. 3, *c* and *f*). At the end of the posterior movement there is a slight anterior shift of the nuclei. Embryos fixed during this movement are in anaphase, telophase, or early interphase (n = 5).

Taking into account the 1–2-min delay before fixation, we estimate from our data that the initial slow movement takes place toward the end of interphase, the fast movement proceeds throughout prophase, and the final slow movement takes place during metaphase and anaphase. The anterior shift of the posterior nuclei occurs during either anaphase or telophase. This phase-specific behavior is the same for both cycles 4 and 5, indicating that this movement is coordinated with the cell cycle. Foe and Alberts (1983) have shown that cortical migration takes place during telophase and early interphase of cycles 8 and 9. Thus, the cell cycle coordination of axial expansion and cortical migration differ.

Cycloheximide Induces Precocious Cortical Migration and Inhibits Axial Expansion

Edgar et al. (1986*a*) blocked transcription with α-amanitin

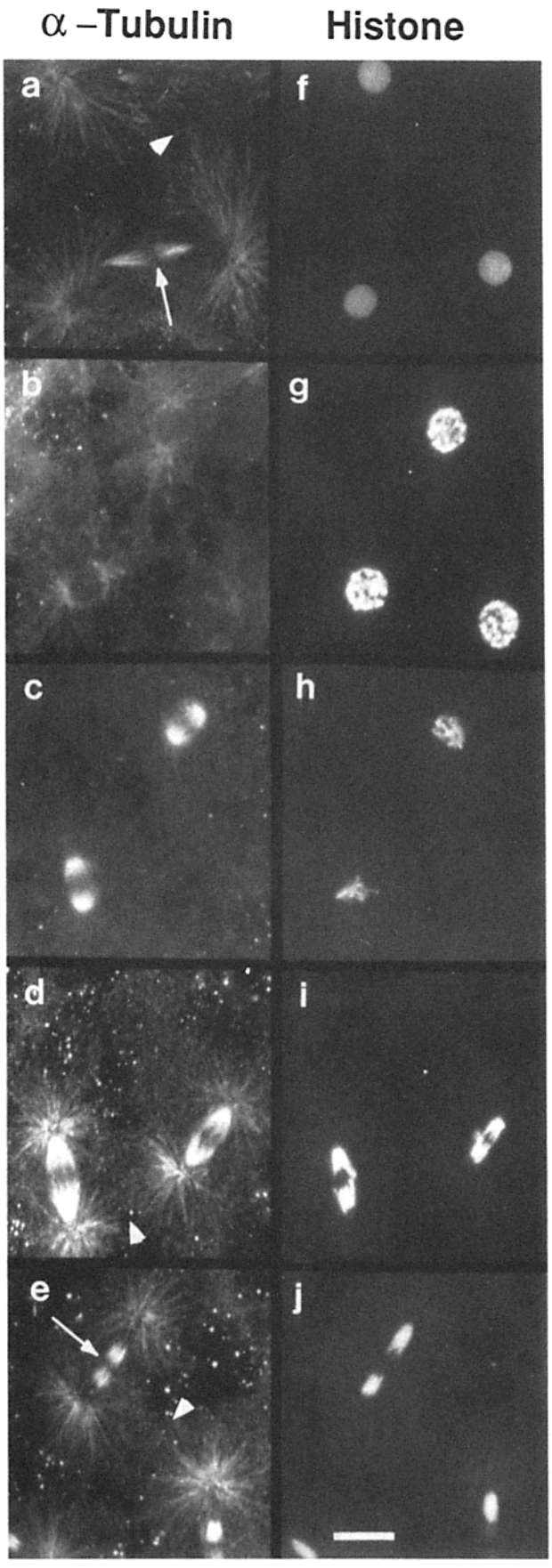

and observed that cortical migration continues. We have repeated this experiment and blocked RNA polymerase II function between cycles 2 and 4 and observed that not only cortical migration but also axial expansion occur at control time and stages (data not shown). However, the requirement for protein synthesis during these movements has not been determined. To address this issue, we have injected embryos with the protein synthesis inhibitor CYH during the premigration divisions and have analyzed nuclear behavior using DIC microscopy. The level of CYH used in these experiments (1 mg/ml) inhibits >95% of the protein synthesis in early embryos. This concentration of CYH also arrests the cell cycle in interphase and inhibits DNA synthesis (Zalokar and Erk, 1976; Edgar and Schubiger, 1986). We obtain results similar to those described below when we inject a fivefold greater concentration of CYH (5 mg/ml). Therefore, we believe that the nuclear movements described below are not a result of a very low level of protein synthesis, although we cannot rule out this possibility.

When embryos are injected with CYH during premigratory stages, the energids pause for 7–10 min and then move synchronously and continuously toward the cortex (n = 6) (Fig. 4, *e–h*). As seen from fixed material, the majority of nuclei migrate to the cortex but, in some cases, two or three nuclei remain in the center of the embryo, reminiscent of yolk nuclei in control embryos. We observe a greater number of embryos with yolk nuclei among those injected with CYH at 65 ± 5 min after egg deposition (AED) (cycles 6–7) than those injected at 45 ± 5 min AED (cycles 4–5) (data not shown). The nuclei move at an average rate of 8.9 μm/min (SD = 1.12, n = 10 nuclei; 3 embryos). This rate is not significantly different from the rate of cortical movement during cycles 8 and 9 in uninjected control embryos (n_{expt} = 9 nuclei; n_{con} = 12 nuclei; P = 0.69), suggesting that these movements might be mechanistically similar. Based on our video observations CYH does not necessarily arrest the cell cycle immediately and the nuclei may undergo one, but not more than two, divisions after CYH injection. This may account for the delay before the initiation of nuclear movements.

We have quantified the time required to complete nuclear migration in CYH-injected embryos. Using DIC microscopy, we have followed live embryos after injection at 45 ± 5 min AED with CYH and find that the nuclei reach the cortex prematurely (Fig. 4). In these CYH-injected embryos, the nuclei reach the cortex at an average of 85.7 min AED (SD = 6.95; n = 20 embryos) whereas nuclei in buffer in-

Figure 5. Cell-cycle changes in microtubule configuration of early embryos (cycles 5 and 6). Each panel shows a planar projection of five optical sections taken at 1-μm intervals with a scanning confocal microscope. The embryos were double labeled with antibodies against α-tubulin (*a–e*) and histones (*f–j*). In early interphase (*a* and *f*), astral microtubules are well established and interdigitate with adjacent nuclei (*arrowhead*), generating a network. The midbody (*long arrows*), which is a remnant of the mitotic spindle, indicates the plane of the previous division. Microtubules begin to break down during prophase (*b* and *g*) until they are almost absent during metaphase (*c* and *h*). During anaphase (*d* and *i*), and continuing through telophase (*e* and *j*), the astral microtubules increase in length and begin to make connections (*arrowhead*) with other nuclei, re-establishing the network. Bar, 10 μm.

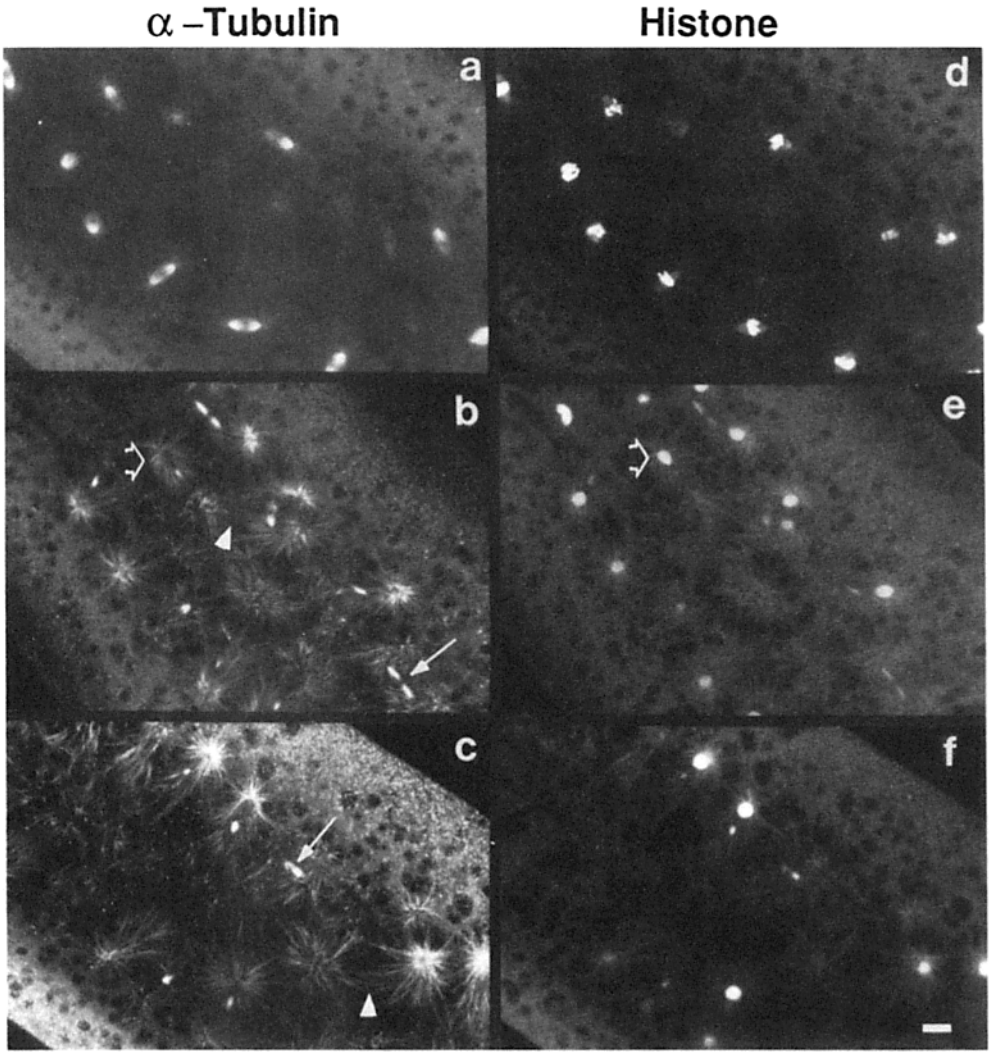

Figure 6. Microtubule reorganization at cycle 7, is correlated with the initiation of cortical migration. At metaphase of cycle 7 (*a* and *d*), the nuclei are distributed along the anterior-posterior axis. There is no evidence for cortical migration during this cell-cycle phase. The astral microtubules are relatively short (*a*) and the nuclei are equidistant from the cortex (*d*). These astral microtubules elongate asymmetrically during telophase (*b* and *e*) such that the microtubules are longer toward the center of the embryo than toward the cortex and begin to interdigitate (*arrowhead*) with the internal yolk nuclei (*open arrow*). The nuclei are displaced relative to the midbody (*long arrows*) indicating that migration has begun (*b* and *e*). (There is limited bleed through of the FITC signal into the RITC channel such that portions of midbody can be seen in the histone image). This asymmetry of the microtubules is pronounced during early interphase (*c* and *f*) where microtubules not only interact with microtubules of laterally adjacent nuclei but also with those of nuclei on the opposite side of the midline. Nuclei are closer to the cortex (compare *e* and *f*), indicating that migration is in progress. Each panel represents a linear projection of confocal micrographs, and the embryos are double labeled, as described in Fig. 5. Anterior is toward the upper left corner. Bar, 10 μm.

jected control embryos reach the cortex at an average of 95.7 min AED (SD = 11.01; n = 9 embryos). In both buffer injected or uninjected control embryos, nuclei migrate only during specific phases of the cell cycle. Also, in buffer injected embryos migration is not observed until nuclear cycle 7, 20–30 min after cycle 5. In contrast, cortical movement in CYH-injected embryos is continuous and is initiated 7–10 min after injection, thus nuclear migration is completed earlier than in control embryos.

While CYH injection does not inhibit cortical migration, it appears to block axial expansion. In embryos that have been injected with CYH before axial expansion (45 min AED) nuclei arrive at the cortex before they extend to the poles such that they occupy a region at the surface that is reminiscent of the position of the nuclear domain in the embryo at the time of injection (Fig. 4). The nuclei migrate outwards isotopically and axial expansion fails to occur. This indicates that axial expansion requires protein synthesis, or cannot proceed while the nuclei are arrested in interphase. This result lends further support to the conclusion that axial expansion and cortical migration are mechanistically distinct.

Role of Microtubules in Nuclear Movement

Inhibitor studies suggest that microtubules play a role in cortical migration (Zalokar and Erk, 1976). However, the organization of microtubules during the preblastoderm cycles has not been reported. Therefore we have used indirect immunofluorescence and laser scanning confocal microscopy to examine microtubule organization in early embryos. Even before nuclear migration begins the microtubule organization is extremely dynamic. An extensive network of interdigitating astral microtubules forms during telophase and early interphase of each cycle, and this network breaks down at each metaphase (Fig. 5).

As observed in cycles 4, 5, and 6, the microtubule network is essentially absent during metaphase of the cortical migration cycles 7, 8, and 9 (Fig. 6 *a*). However, the astral arrays appear longer and more prominent during these migratory cycles than those seen during cycles 4, 5, and 6. During late telophase and early interphase, when the nuclei are moving toward the cortex (Foe and Alberts, 1983), microtubules extending toward the cortex are short and do not reach the surface of the embryo. On the other hand, those extending to-

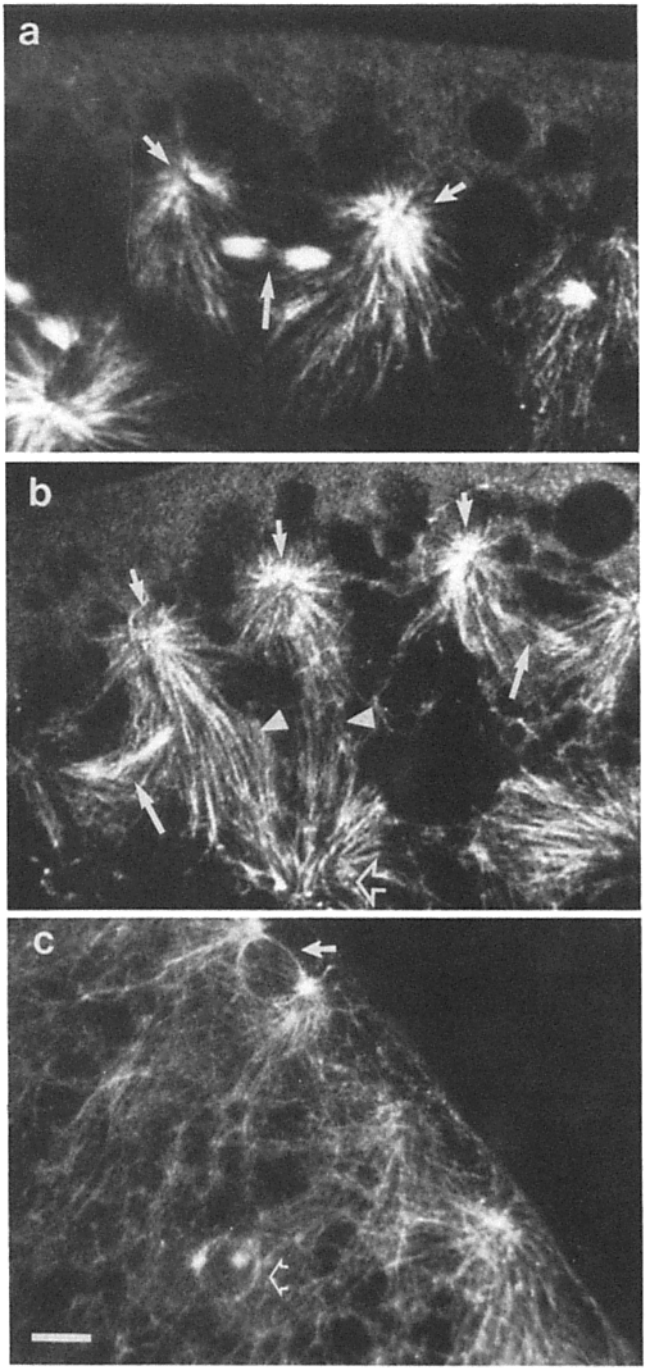

Figure 7. Microtubule reorganization at cycle 9, during cortical migration. (*a*) Microtubule distribution at the onset of cortical migration, during early telophase of nuclear cycle 9. The nuclei (*short arrows*) are displaced slightly relative to the midbody (*long arrows*), indicating that cortical movement has begun. Microtubules extending into the embryo are significantly longer than those directed toward the surface. (*b*) Microtubule distribution during the cortical movements of late telophase of nuclear cycle 9. The nuclei (*short arrows*) are well ahead of the midbody (*long arrows*), indicating that cortical migration is in progress. Bundles of interdigitating microtubules (*arrowheads*) link the migrating nuclei with the internal yolk nuclei (*open arrow*). (*c*) Microtubule network at the completion of nuclear migration. An extensive mesh of microtubules extends from the microtubule organizing center associated with the cortical nuclei into the embryo. The antiparallel microtubule arrays present during migration are not observed. Each panel represents a planar projection of confocal micrographs of embryos labeled only with anti-α-tubulin, prepared as described in Fig. 5. Bar, 10 μm.

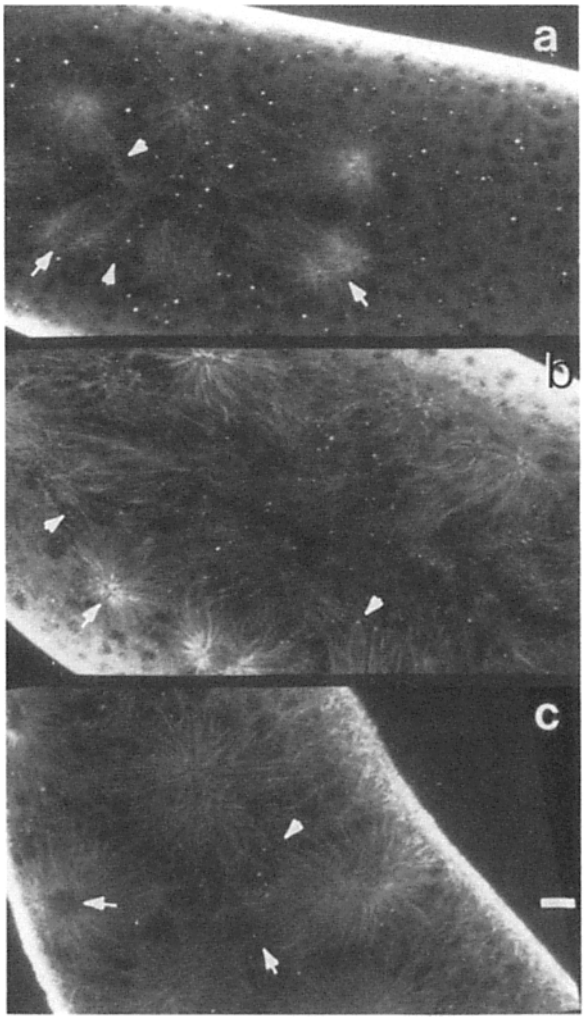

Figure 8. Microtubule organization after injection of cycloheximide. Embryos were stained with anti-α-tubulin after the injection of CYH. (*a*) 10 min after injection the microtubules extend inward to the center of the embryo, where they interdigitate (*arrowheads*) with the microtubules of other nuclei as the nuclei (*short arrows*) move outward. (*b*) By 20 min after injection this extensive asymmetric polymerization of microtubules has continued until the nuclei approach the cortex by (*c*) 30 min after injection. This asymmetric polymerization resembles that of early interphase migrating nuclei of control embryos (Fig. 6 *c*). Each panel represents a planar projection of confocal micrographs, prepared as described in Fig. 5. Bar, 10 μm.

ward the center of the embryo are much longer and can form anti-parallel arrays with microtubules originating at the yolk nuclei and with microtubules associated with nuclei migrating toward the opposite side of the embryo (Fig. 6, *b* and *c* and Fig. 7, *a* and *b*). Microtubules of adjacent nuclei also appear to interact (Figs. 6 *c* and 7 *b*). As the embryo proceeds into interphase, the length asymmetry between microtubules directed toward and away from the cortex remains pronounced, but the antiparallel arrays are no longer observed (Fig. 7 *c*). These observations are not consistent with models in which nuclei are pulled to the cortex by a microtubule-dependent mechanism (Wolf, 1980).

If cortical migration in CYH-injected embryos is related to migration in control embryos, and interacting microtubules are important for cortical migration, then the microtu-

bule configuration in CYH-injected embryos should mimic that of migrating nuclei in uninjected embryos. The microtubule organization typical of that found in a CYH-injected embryo is shown in Fig. 8. The asymmetry of microtubule length and the extensive interactions between microtubules from neighboring nuclei are similar to that observed in control embryos, although the microtubule arrays are longer and appear to contain more microtubules than those found in uninjected embryos (compare Figs. 6 and 8) or in buffer injected control embryos. By 75 ± 5 min AED the diameter of the microtubule array of the energids of CYH-injected embryos is significantly larger than those of buffer injected control interphase nuclei (n_{expt} = 58 energids from 10 embryos; x_{expt} = 50.33 ± 9.5 μm; n_{con} = 60 energids from 6 embryos, x_{con} = 24.56 ± 4.6 μm; P = 0.001) as measured in single confocal optical sections using the Bio Rad COMOS software (Bio Rad Labs., Hercules, CA). In addition, nuclear migration in CYH-injected embryos is prevented by the microtubule inhibitor colcemid (data not shown). This result further supports the conclusion that cortical migration in CYH-injected embryos requires microtubule function. Since cortical migration in CYH-injected and control embryos is similar in microtubule organization, rate, and microtubule function dependency, we conclude that the CYH-injected embryos rely on the same force-generating machinery as the control embryos.

Discussion

Posterior and Cortical Nuclear Movements Proceed via Different Mechanisms

Two major nuclear movements, which we term axial expansion and cortical migration, are required for normal *Drosophila* blastoderm formation. Previous pharmacological studies (Zalokar and Erk, 1976) indicate that axial expansion depends on actin function while cortical migration depends on microtubules function. Additionally, we show that axial expansion differs from cortical migration in rate, cell-cycle dependency, and the requirement for protein synthesis. These observations clearly demonstrate that, in *Drosophila*, axial expansion and cortical migration are mechanistically distinct, as postulated by Wolf (1980) for the gall midge.

The cytochalasin B sensitivity of the axial expansion suggests that actin plays an important role in this movement (Zalokar and Erk, 1979; Hatanaka and Okada, 1991). Hatanaka and Okada (1991) have described a maternal-effect mutation, *gs (l)N26*, in which normal axial expansion is inhibited, but cortical migration proceeds. They attribute this phenotype to defects in the microfilaments, although the structural basis of this actin-dependent force is not understood. Axial expansion is not sensitive to colcemid, suggesting that microtubules do not perform a major role in this movement (Zalokar and Erk, 1976; Hatanaka and Okada, 1991). Supporting this hypothesis, we find that axial expansion occurs during prophase and prometaphase, phases of the cell cycle when the microtubule network is breaking down.

Regulation of Cortical Migration

Cortical migration is composed of a series of stepwise movements that begin during nuclear cycles 7, 8, and 9, and are complete at interphase of nuclear cycle 10. What triggers the onset of these remarkably reproducible movements? Neither axial expansion (data not shown) nor cortical migration (Edgar et al., 1986*a*) are inhibited by the injection of α-amanitin, indicating that zygotic transcription is not required for force generation during these movements or to regulate its onset. We demonstrate that nuclei migrate to the cortex in CYH-injected embryos, suggesting that new protein synthesis is not required to generate the forces that drive nuclei to the cortex. CYH injection induces premature cortical migration, suggesting that the onset of cortical migration may be regulated (repressed) by the synthesis of a specific protein or proteins. This raises the possibility that the onset of this movement is normally triggered by loss of a maternally supplied message that encodes this hypothetical repressor. We postulate that because these nuclei do not pause to mitose they have more time than control nuclei to move toward the cortex, possibly explaining the observation that nuclei in CYH-injected embryos reach the cortex before their control counterparts. Furthermore, migration in CYH-injected embryos is not blocked by aphidicolin (data not shown), indicating that DNA synthesis is not likely to trigger cortical migration.

Previous studies suggest that microtubules play a role in generating the force required for cortical migration (Zalokar and Erk, 1976). How might microtubules mediate cortical migration? Wolf (1980) has proposed that microtubules link the nuclei with the cortex and that nuclei are pulled to the surface by a force transduced by these microtubules. However, we do not observe microtubules linking the migrating nuclei with the cortex, suggesting that for *Drosophila* this model is incorrect. Instead, we observe a dynamic microtubule network that interconnects the migrating nuclei. Cell-cycle changes in the microtubule cytoskeleton correlate with the cell-cycle dependence of cortical migration: anti-parallel microtubule arrays interconnect the nuclei during nuclear movement, whereas these arrays break down during the nonmigratory phases of late interphase, prophase, and metaphase. Also, cortical migration in CYH-injected embryos is accompanied by the assembly of a microtubule network that is morphologically similar to that observed during normal migration. It is possible that these changes are the result, rather than the cause, of cortical migration. However, such an assumption requires that novel proteins are produced to mediate cortical migration. The most parsimonious interpretation of our observations is that microtubule-dependent forces push nuclei away from one another, and that these repulsive forces drive nuclei toward the surface (Fig. 9).

A Model for Cortical Migration

In this model, the force driving cortical migration is produced by a plus-end directed microtubule motor, acting between antiparallel microtubules. This means of force generation is attractive because it does not invoke a novel motile mechanism. The antiparallel interactions that we propose to drive nuclear migration are conceptually identical to those which produce anaphase B movements during mitosis. Thus, the machinery for cortical movement could simply shift from the depolymerizing spindle microtubules to the newly formed astral microtubules.

To identify the functional control mechanisms of nuclear movements, detailed analyses of maternal-effect mutations

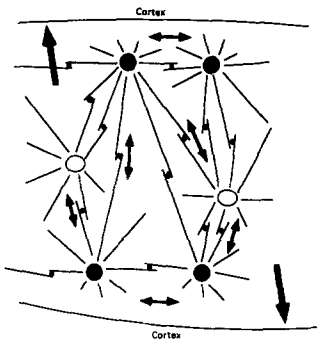

Figure 9. Model of cortical migration. The large black circles represent migrating nuclei while the white circles represent yolk nuclei. Lines show interconnecting microtubules with the small black dots indicating where putative plus-end-directed motors might be located. The double-ended arrows illustrate how the antiparallel microtubules could push against each other, generating an outward force, which is depicted by heavy arrows.

should elucidate specific gene products required for these movements. The phenotypes of such mutations have been described as "mid-cleavage crises" (Counce, 1973). The maternal-effect mutation *gs(l)N26* appears to represent one such mutation. Embryos from homozygote *gs(l)N26* mothers exhibit defective axial extension, but normal cortical migration. A second class of maternal effect mutations, whose embryos exhibit normal axial expansion but lack cortical migration, is also expected. In embryos from heterozygous *Laborc* mothers the nuclei extend posteriorly but do not reach the cortex (Szabad, personal communication). Further detailed analyses of maternal-effect mutations may reveal more of these types of mutations, and their analysis should lend insight into the molecular mechanisms of these two nuclear movements.

We would like to thank Mark Kirschner, Mark Mooseker, and Greenfield Sluder for stimulating discussions on this work. We would also like to acknowledge the critical reading of the manuscript by Robin Wright, Barbara Wakimoto, Jordan Raff, Victoria Foe, Kelly Owens, Kathleen Wilson, and the members of the Schubiger lab. We thank Paulette Brunner and David Baldwin for technical assistance with the confocal imaging.

This work was supported by National Institutes of Health grants GM33656 to G. Schubiger, PO1 GM31286 and RO1 GM23928 to Dr. Bruce Alberts, and ISO RR4646.

Received for publication 10 February 1993 and in revised form 1 April 1993.

References

Counce, S. J. 1973. The causal analysis of insect embryogenesis. *In* Developmental Systems: Insects. Vol. 2. S. J. Counce and C. H. Waddington, editors. Academic Press, London and New York. 1–156.

Edgar, B. A., and G. Schubiger. 1986. Parameters controlling transcriptional activation during early *Drosophila* development. *Cell.* 44:871–877.

Edgar, B. A., C. P. Kiehle, and G. Schubiger. 1986*a*. Cell cycle control by the nucleocytoplasmic ratio in early *Drosophila* development. *Cell.* 44: 365–372.

Edgar, B. A., M. Weir, G. Schubiger, and T. Kornberg. 1986*b*. Repression and Turnover pattern fushi tarazu RNA in the early *Drosophila* embryo. *Cell.* 44: 747–754.

Edgar, B. A., G. M. Odell, and G. Schubiger. 1987. Cytoarchitecture and the patterning of fushi tarazu expression in the *Drosophila* blastoderm. *Genes & Dev.* 1:1226–1237.

Foe, V. E., and B. M. Alberts. 1983. Studies of nuclear and cytoplasmic behavior during the five mitotic cycles that precede gastrulation in *Drosophila* embryogenesis. *J. Cell Sci.* 61:31–70.

Gard, D. L., S. Hafezi, T. Zhang, and S. Doxsey. 1990. Centrosome duplication continues in cycloheximide-treated *Xenopus* blastulae in the absence of a detectable cell cycle. *J. Cell Biol.* 110:2033–2042.

Hatanaka, K., and M. Okada. 1991. Retarded nuclear migration in *Drosophila* embryos with aberrant F-actin reorganization caused by maternal mutations and by cytochalasin treatment. *Development (Camb.).* 111:909–920.

Karr, T. L., and B. M. Alberts. 1986. Organization of the cytoskeleton in early *Drosophila* embryos. *J. Cell Biol.* 102:1494–1509.

Kellogg, D. R., T. J. Mitchison, and B. M. Alberts. 1988. Behavior of microtubules and actin filaments in living *Drosophila* embryos. *Development (Camb.).* 103:675–687.

Maul, V. V. 1967. Dynamik und Erbverhalten plasmatischer Eibereiche der Honigbiene. *Zool. Jb. Anat.* 84:63–166.

Rabinowitz, M. 1941. Studies on the cytology and early embryology of the egg of *Drosophila melanogaster. J. Morphol.* 69:1–49.

Scriba, M. E. L. 1964. Beeinflussung der frühen Embryonalentwicklung von *Drosophila melanogaster* durch Chromosomenaberrationen. *Zool. Jb. Anat.* 81:435–490.

Sluder, G., F. Miller, and C. Reider. 1986. The reproduction of centrosomes: nuclear versus cytoplasmic controls. *J. Cell Biol.* 103:1873–1881.

Sluder, G., F. J. Miller, R. Cole, and C. Rieder. 1990. Protein synthesis and the cell cycle: centrosome reproduction in sea urchin eggs is not under translational control. *J. Cell Biol.* 110:2025–2032.

Strasburger, E. H. 1934. Uber die Zellbewegungen bei der Eifurchung der Fliege Calliphora erythrocephala Meigen. *Zeitschriff. wissensch. Zoologie.* 145:625–641.

Theurkauf, W. E. 1992. Behavior of structurally divergent α-tubulin isotypes during *Drosophila* embryogenesis. Evidence for post-translational regulation of isotype abundance. *Dev. Biol.* 154:205–217.

Warn, R. M., and A. Warn. 1986. Microtubule arrays present during the syncytial and cellular blastoderm stages of the early *Drosophila* embryo. *Exp. Cell Res.* 163:201–211.

Warn, R. M., R. Magrath, and S. Webb. 1984. Distribution of F-actin during cleavage of the *Drosophila* syncytial blastoderm. *J. Cell Biol.* 98:156–162.

Weir, M. P., B. A. Edgar, T. Kornberg, and G. Schubiger. 1988. Spatial regulation of engrailed expression in the *Drosophila* embryo. *Genes & Dev.* 2: 1194–1203.

Wolf, R. 1980. Migration and division of cleavage nuclei in the gall midge, *Wachtliella persicariae. Wilhelm Roux's Arch.* 188:65–73.

Würgler, F. E., and H. Ulrich. 1976. Radiosensitivity of embryonic stages. *In* The Genetics and Biology of Drosophila. vol. 1c. M. Ashburner and E. Novitski, editors. Academic Press. London and New York. 1269–1298.

Yasuda, G. K., J. Baker, and G. Schubiger. 1991. Independent roles of centrosomes and DNA in organizing the *Drosophila* cytoskeleton. *Development (Camb.).* 111:379–391.

Zalokar, M., and I. Erk. 1976. Division and migration of nuclei during early embryogenesis of *Drosophila melanogaster. J. Mic. Biol. Cell.* 23:97–106.